High-performance ionic liquid-based microextraction method (ILBME) for the trace determination of paroxetine as a pharmaceutical pollutant in environmental and biological samples

Mehdi Hosseini*[a]

Department of Chemistry, Faculty of Basic Sciences, Ayatollah Boroujerdi University, Boroujerd, Iran.

Supplementary Information

Table S1 Determined physical properties of [Hibmim][Cl] (*n=3*)

Properties	Density, g mL^{-1}	Refractive index	Boiling point, ˚C	Melting point, ˚C	Freezing point, ˚C
Value	1.54±0.05	1.35±0.1	274±0.1	52±0.05	-16±0.1

Table S2 Elemental analysis of ionic liquid of [Hibmim][Cl]

Compound	Founded (expected) (%)				
	C	H	N	O	Cl
[Hibmim][Cl]	53.28 (53.32)	8.92 (8.95)	16.90 (16.96)	6.43 (6.46)	14.29 (14.31)

Table S3 Elemental analysis of {paroxetine-[Hibmim][Cl} chelate

Compound	Founded (expected) (%)					
	C	H	N	O	F	Cl
{paroxetine-[Hibmim][Cl]}	62.20 (62.43)	7.30 (7.34)	9.68 (9.71)	11.00 (11.09)	3.27 (3.29)	6.00 (6.14)

Table S4 Interaction energies (ΔE_{int}) and Gibbs free energies ($\Delta G_{int)}$ for various interactions of **ionic** liquid and paroxetine

Entry	interaction	E_{cmpx} (a.u.)	ΔE_{int} (kJ/mol)	G_{cmpx} (a.u.)	ΔG_{int} (kJ mol^{-1})
1	O3…H12	-2208.82346	-56.5375	-2208.22492	3.310756
2	H4…N13 N1…H12	-2208.82077	-49.4775	-2208.22778	-4.20605
3	H2…N13	-2208.83161	-77.9196	-2208.23459	-22.0857
4	H…π (ring) Cl5…H12)	-2208.84446	-111.681	-2208.24252	-42.9059
5	H4…O15 Cl5…H12	-2208.84910	-123.847	-2208.24398	-46.7392
6	H2…O15	-2208.84219	-105.708	-2208.23707	-28.6074
7	H2…F14 Cl5…H12	-2208.83625	-90.1255	-2208.23834	-31.9235

Table S-5 Comparison of various counter ions used as phase separation agents (*n=3*)

Counter ion	Extraction efficiency of paroxetine (%)
PF_6^-	98.6±1.9
NTF_2^-	98.2±2.2
BF_4^-	89.7±2.0

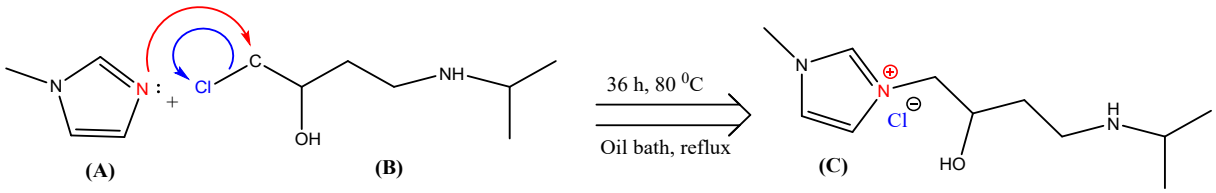

Fig. S1 The synthesis route of the 3-(2-hydroxy-4-(isopropylamino)butyl)-1-methylmidazolium chloride ([Hibmim][Cl]).

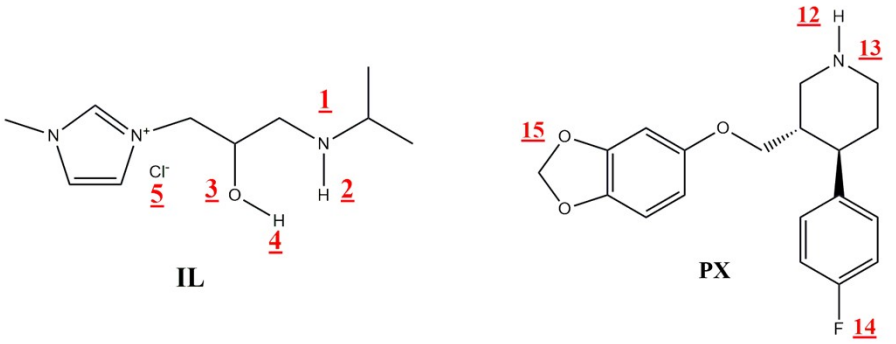

Fig. S2 The optimized geometries of paroxetine (PX) and the ionic liquid (IL) using the M06-2X functional and the 6-31G(d,p) basis set.

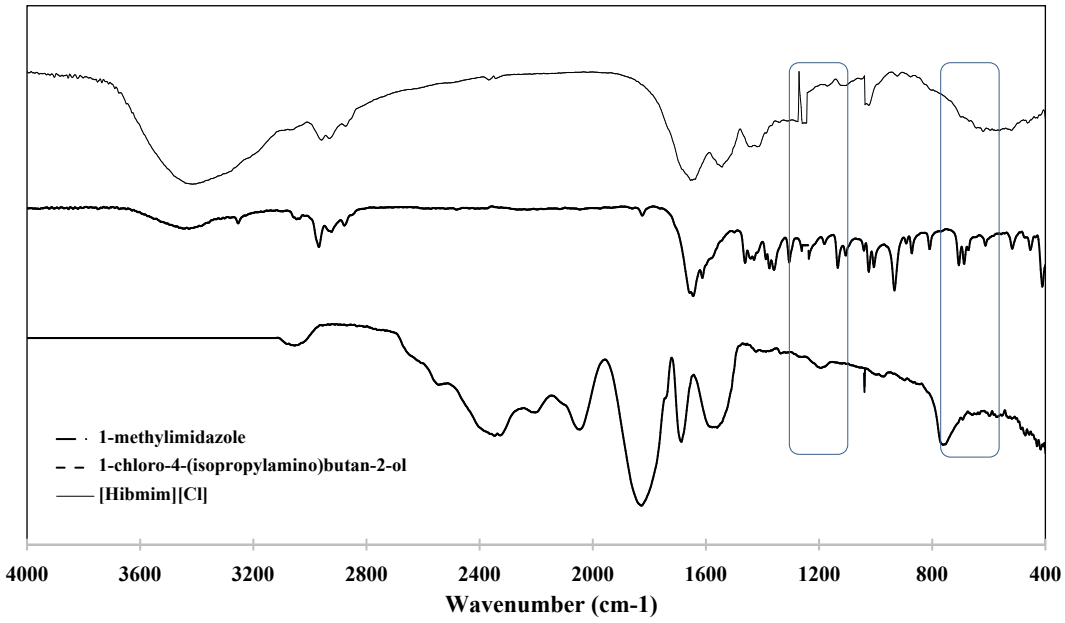

Fig. S3 FTIR spectra for the raw materials and the resulting ionic liquid [Hibmim][Cl].

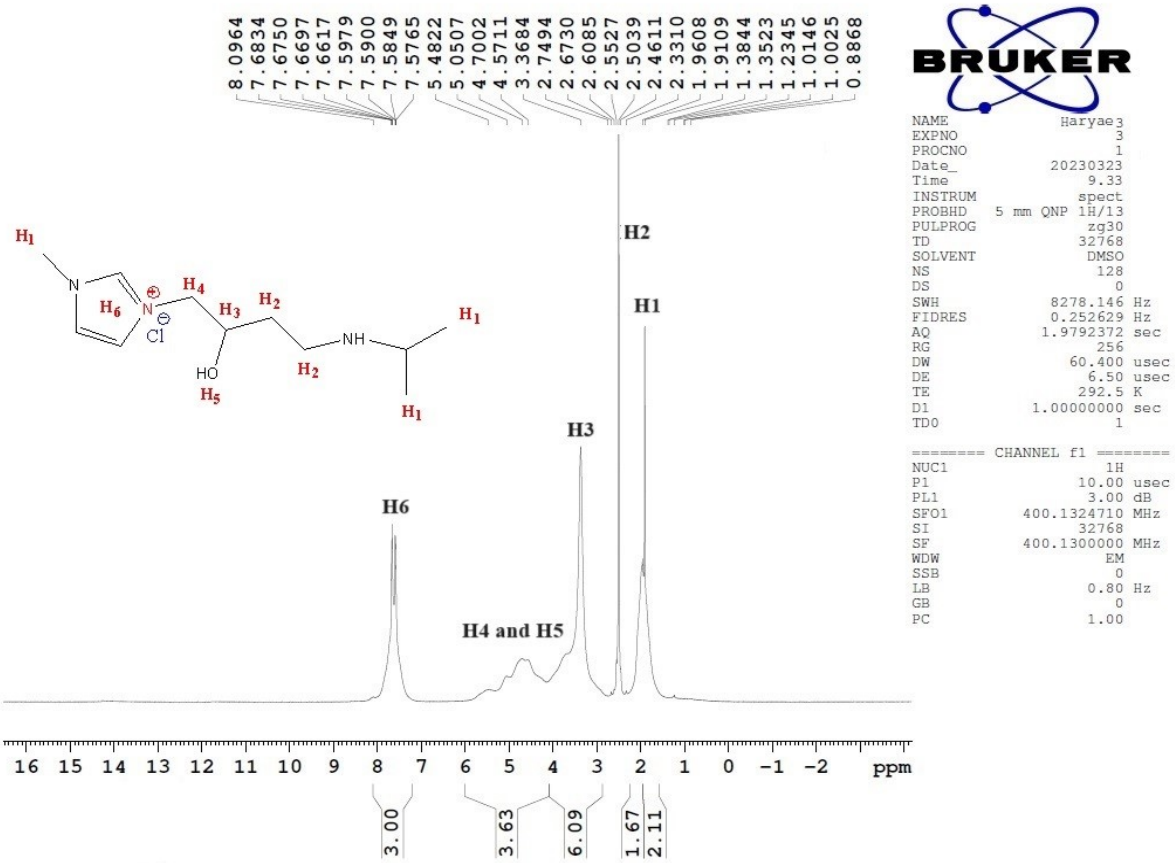

Fig. S4 HNMR of ionic liquid of [Hibmim][Cl].

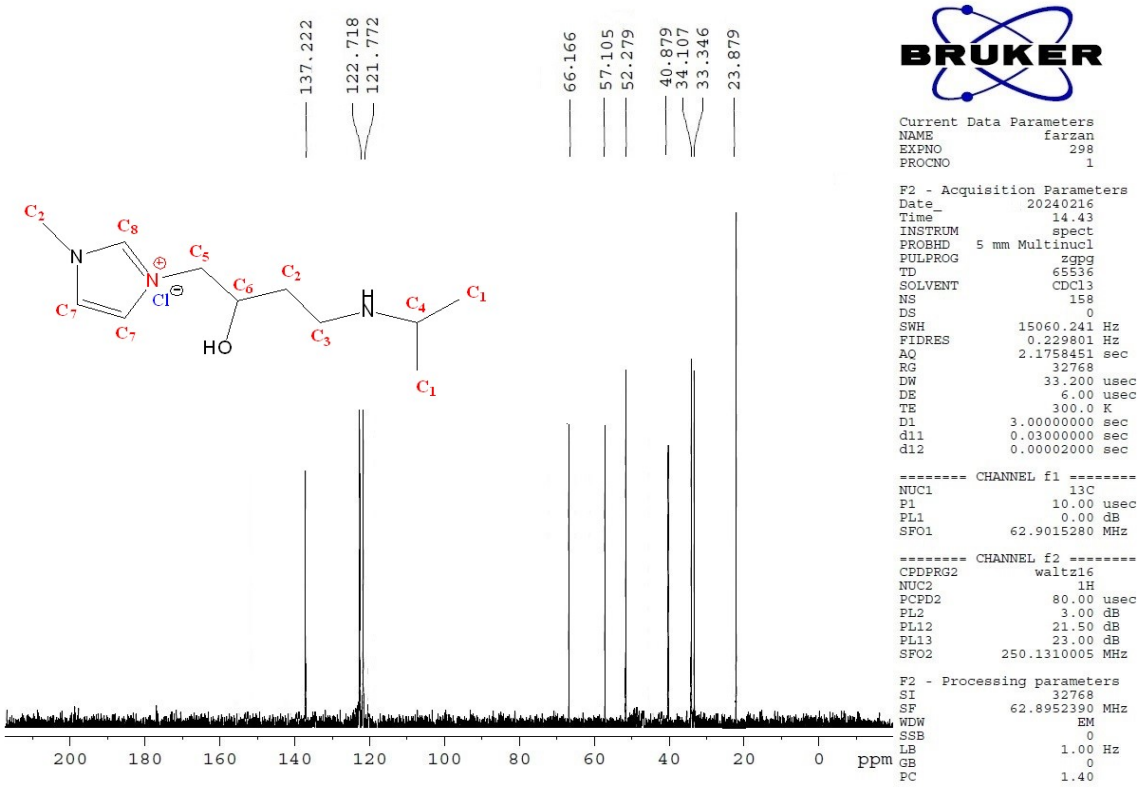

Fig. S5 CNMR of ionic liquid of [Hibmim][Cl].

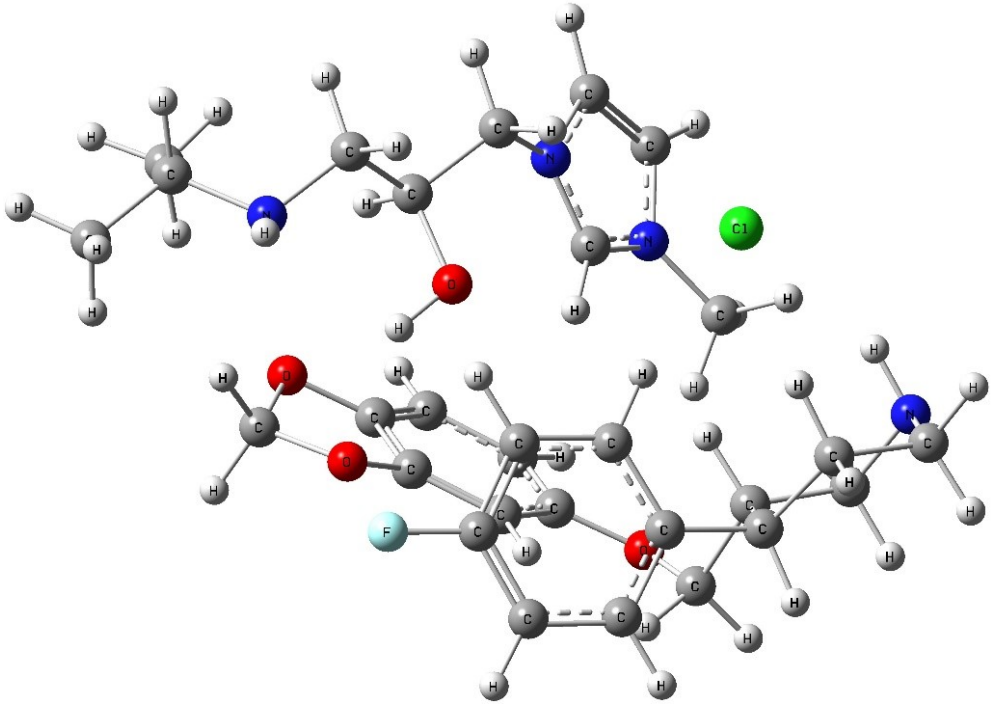

Fig. S6 The optimized geometry of most stable complex between ionic liquid and paroxetine.

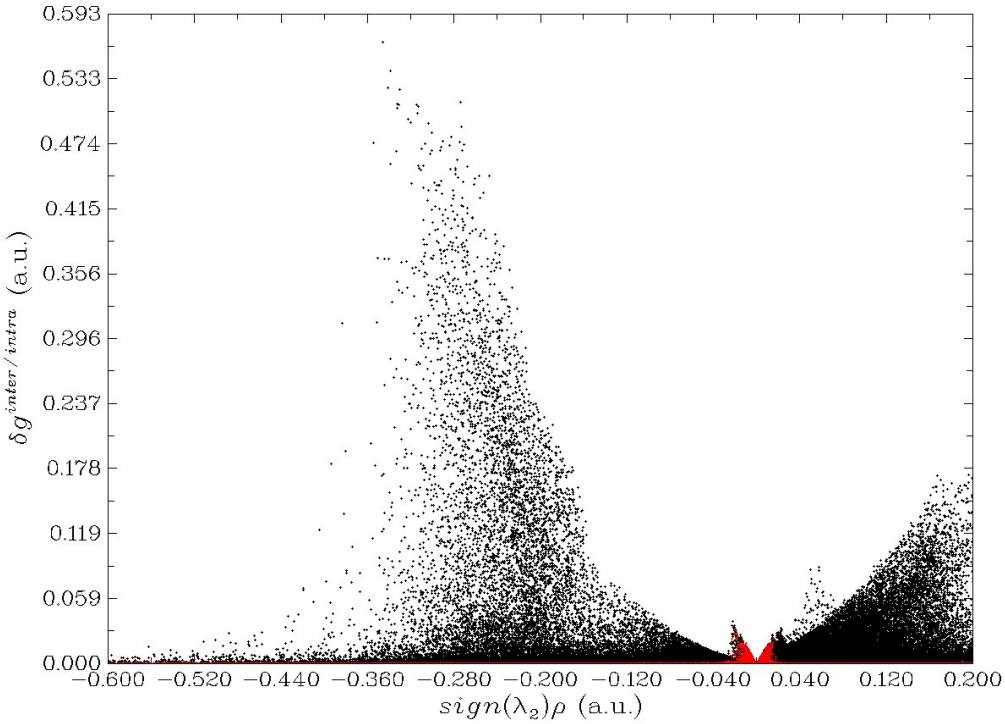

Fig. S7 The different values of isosurface δg function and sign (λ2)ρ.

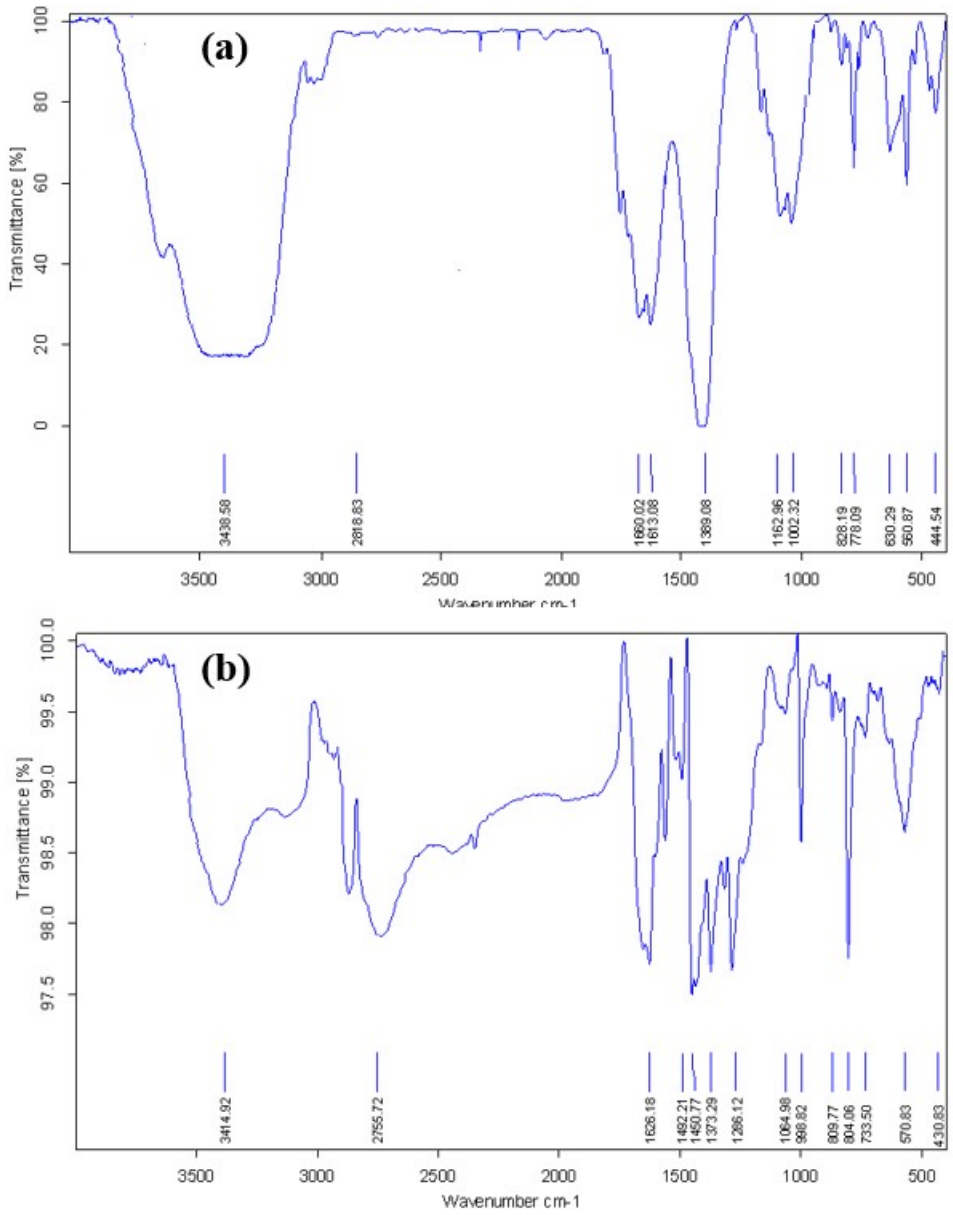

Fig. S8 FTIR spectra for (a) paroxetine before extraction and (b) complexed paroxetine after extraction.

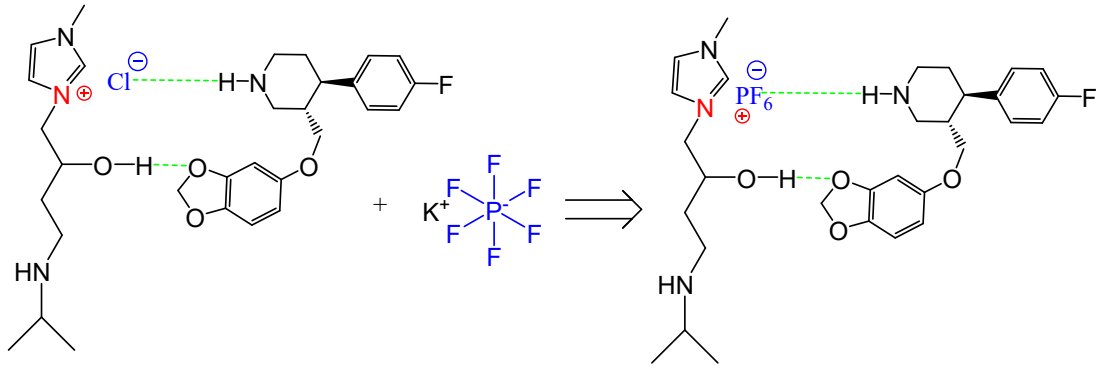

Hydrophilic complex of {paroxetine-[Hibmim][Cl]

Hydrophobic complex of {paroxetine-[Hibmim][PF_6]

Fig. S9 The change in polarity from the hydrophilic chelate {paroxetine-[Hibmim][Cl]} to the hydrophobic chelate {paroxetine-[Hibmim][PF_6]}.

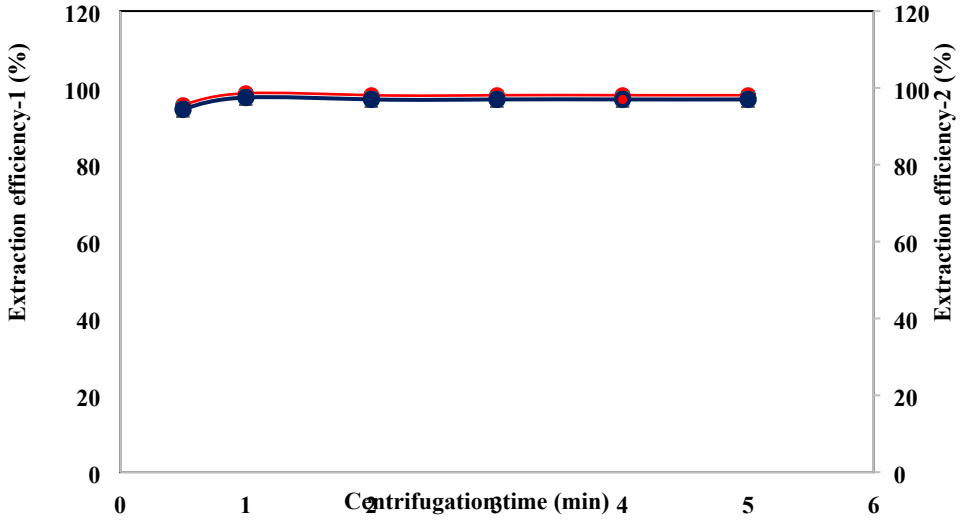

Fig. S10 The effect centrifugation time on the extraction efficiency of paroxetine. Investigated conditions: varying centrifugation time, pH of 7.0, 100 mg of IL, 75 mg of PF_6^-, 20,000 mg L^{-1} of NaCl and centrifugation at 2000 rpm.

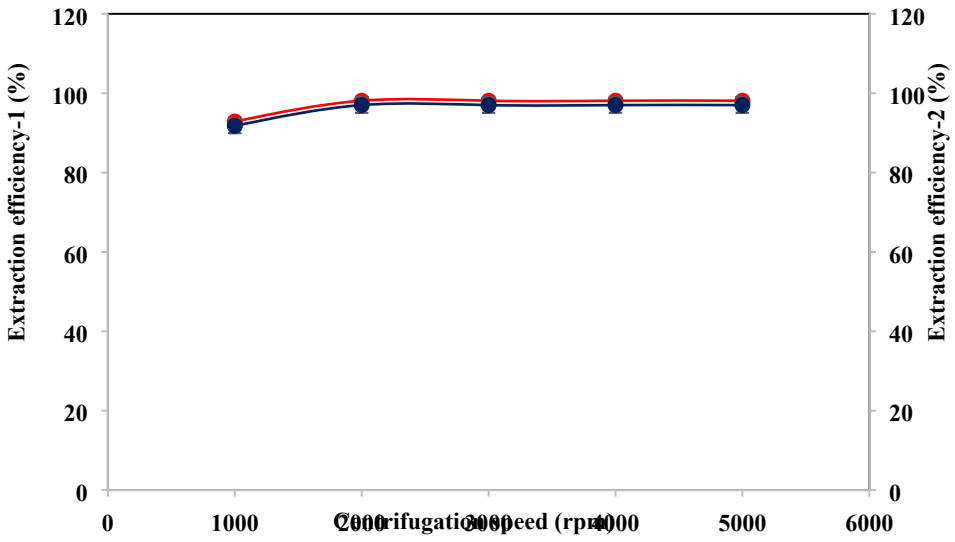

Fig. S11 The effect centrifugation speed on the extraction efficiency of paroxetine. Investigated conditions: varying centrifugation speed, pH of 7.0, 100 mg of IL, 75 mg of PF_6^-, 20,000 mg L^{-1} of NaCl and centrifugation for 1 min. (B) The effect of ionic

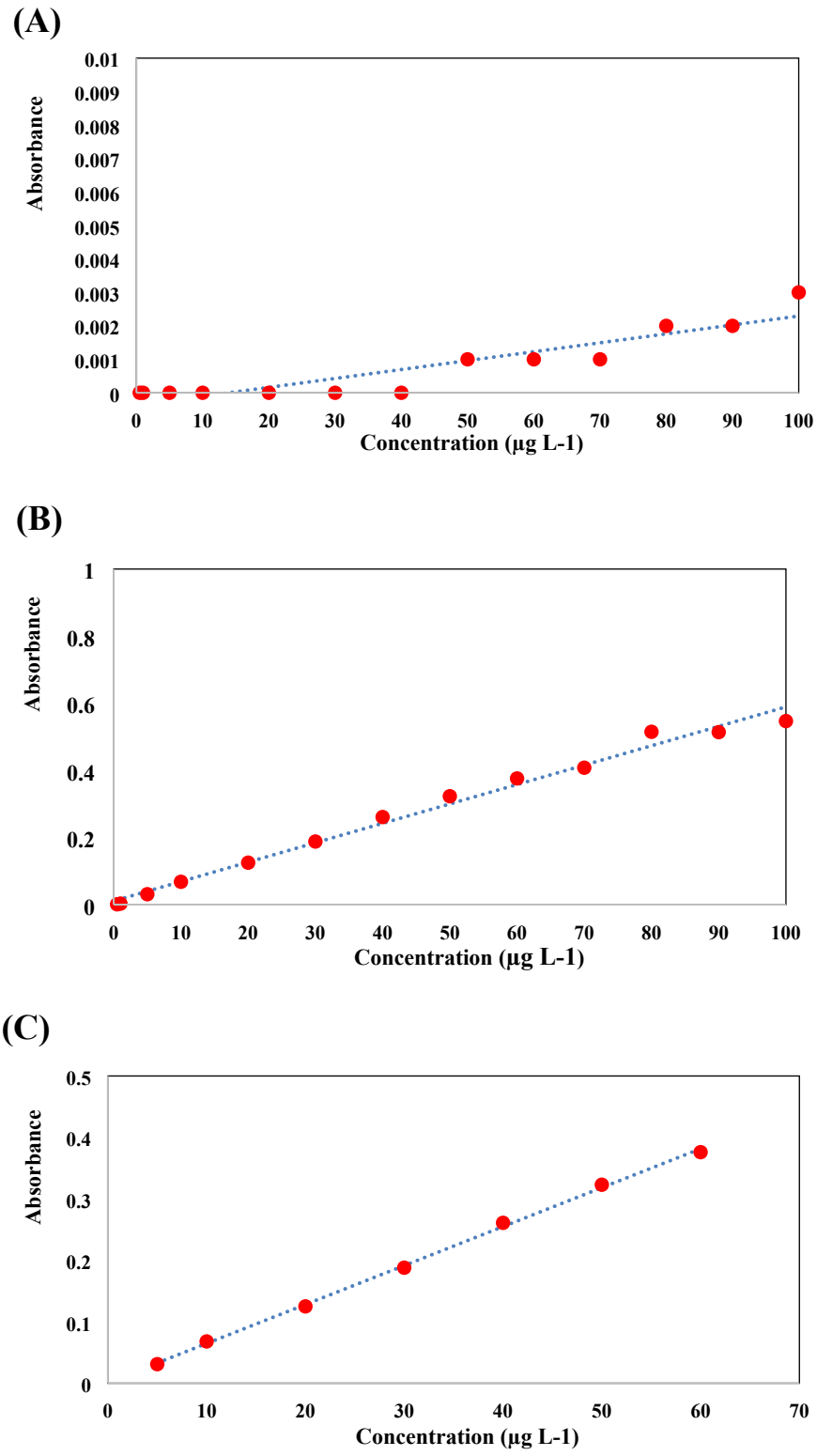

Fig. S12 (A) The calibration curve before microextraction, (B) after microextraction, and (C) the estimated LDR.